(19) Europäisches Patentamt
European Patent Office
Office européen des brevets

(11) EP 3 006 055 B1

(12) **EUROPEAN PATENT SPECIFICATION**

(45) Date of publication and mention of the grant of the patent:
19.02.2020 Bulletin 2020/08

(21) Application number: **14188556.6**

(22) Date of filing: **10.10.2014**

(51) Int Cl.:
A61L 27/50 *(2006.01)* ***A61L 27/36*** *(2006.01)*
A61B 5/00 *(2006.01)* ***A61N 1/05*** *(2006.01)*
A61B 5/04 *(2006.01)*

(54) **Improved biomaterials for neuronal implants and use of said biomaterials in the diagnosis and therapy of neuronal diseases**

Verbesserte Biomaterialien für neuronale Implantate und Verwendung der besagten Biomaterialien in der Diagnose und Therapie von neuronalen Erkrankungen

Biomatériaux améliorés pour implants neuronaux et utilisation desdits biomatériaux dans le diagnostic et la thérapie de maladies neuronales

(84) Designated Contracting States:
AL AT BE BG CH CY CZ DE DK EE ES FI FR GB GR HR HU IE IS IT LI LT LU LV MC MK MT NL NO PL PT RO RS SE SI SK SM TR

(43) Date of publication of application:
13.04.2016 Bulletin 2016/15

(73) Proprietor: **Albert-Ludwigs-Universität Freiburg**
79085 Freiburg (DE)

(72) Inventors:
- **SHASTRI, Prasad**
  79206 Breisach (DE)
- **BLUMENTHAL, Nils R.**
  22765 Hamburg (DE)

(74) Representative: **Krauss, Jan**
Boehmert & Boehmert
Anwaltspartnerschaft mbB
Pettenkoferstrasse 22
80336 München (DE)

(56) References cited:
WO-A1-2014/116132 **WO-A2-2006/014493**
US-A1- 2007 038 307

- **PENNISI CP; DOLATSHAHI-PIROUZ A; FOSS M; CHEVALLIER J; FINK T; ZACHAR V; BESENBACHER F; YOSHIDA K.: "Nanoscale topography reduces fibroblast growth, focal adhesion size and migration-related gene expression on platinum surfaces", COLLOIDS SURF B BIOINTERFACES, vol. 85, no. 2, 26 February 2011 (2011-02-26), pages 189-97, XP002737425,**
- **SUCHYNA T M ET AL: "BILAYER-DEPENDENT INHIBITION OF MECHANOSENSITIVE CHANNELS BY NEUROACTIVE PEPTIDE ENANTIOMERS", NATURE, NATURE PUBLISHING GROUP, UNITED KINGDOM, vol. 430, no. 6996, 8 July 2004 (2004-07-08), pages 235-240, XP001203671, ISSN: 0028-0836, DOI: 10.1038/NATURE02743**
- **SATOH K ET AL: "A novel membrane protein, encoded by the gene covering KIAA0233, is transcriptionally induced in senile plaque-associated astrocytes", BRAIN RESEARCH, ELSEVIER, AMSTERDAM, NL, vol. 1108, no. 1, 7 September 2006 (2006-09-07), pages 19-27, XP027955178, ISSN: 0006-8993 [retrieved on 2006-09-07]**
- **D. T. THEODOSIS ET AL: "Activity-Dependent Structural and Functional Plasticity of Astrocyte-Neuron Interactions", PHYSIOLOGICAL REVIEWS, vol. 88, no. 3, 1 July 2008 (2008-07-01), pages 983-1008, XP055196547, ISSN: 0031-9333, DOI: 10.1152/physrev.00036.2007**

Printed by Jouve, 75001 PARIS (FR)

(Cont. next page)

- **NILS R. BLUMENTHAL ET AL: "Stochastic nanoroughness modulates neuron-astrocyte interactions and function via mechanosensing cation channels", PROCEEDINGS OF THE NATIONAL ACADEMY OF SCIENCES, vol. 111, no. 45, 27 October 2014 (2014-10-27), pages 16124-16129, XP055196480, ISSN: 0027-8424, DOI: 10.1073/pnas.1412740111 & Nils R. Blumenthal ET AL: "Supporting Information: Stochastic nanoroughness modulates neuron-astrocyte interactions and function via mechanosensing cation channels", Proceedings of the National Academy of Sciences, vol. 111, no. 45, 27 October 2014 (2014-10-27), pages 16124-16129, XP055196483, ISSN: 0027-8424, DOI: 10.1073/pnas.1412740111**
- **Luca Ferrarini ET AL: "Morphological Hippocampal Markers for Automated Detection of Alzheimer's Disease and Mild Cognitive Impairment Converters in Magnetic Resonance Images", JOURNAL OF ALZHEIMER'S DISEASE, vol. 17, no. 3, 1 July 2009 (2009-07-01), pages 643-659, XP055370852, NL ISSN: 1387-2877, DOI: 10.3233/JAD-2009-1082**

Description

[0001] The present invention relates to a neural implant comprising a biomaterial having an outer surface with a stochastic nanoroughness (Rq), and the application of said stochastic nanoroughness in preventing glial scars.

[0002] Controlling cellular responses on biomaterial surfaces is crucial in biomedical applications such as tissue engineering and implantable prosthetics. Since cells encounter various nanoscale topographic features in their natural environment, it has been postulated that surface nanotopography may be an alternative route to fabricate biomaterials with a desirable cellular response.

[0003] Engineered surfaces are created in various ways, typically by machining, surface treatment and coating. Most often a combination of various machining, treatment and coating operation are used to produce surfaces with characteristics that are desirable for particular application. Each surface generation process produces surface topography characteristic of the process and process variables used. Surface topography, therefore, contains signature of the surface generation process and as such can be used to diagnose, monitor and control the manufacturing process. Surface topography establishes a correspondence between an engineering surface phenomenon (e.g. wear, chatter, etc.) and its topographical characteristics (e.g. bearing area, oil retention volume etc.). A surface profile may be composed of a range of frequency components. The high frequency (or short wave) components correspond to those that are perceived to be rough and hence called "roughness". The low frequency (or long wave) components correspond to more gradual changes in the profile and are often associated with the terms "waviness" or even "form". The waviness or the low frequency component is periodic in nature, while the high frequency component or the roughness is random. Different frequency components in a surface profile can be separated out by a procedure called as filtering. The random surface roughness is the characteristic of any machining process and is characterized by many amplitude and statistical parameters.

[0004] Lipski et al. (in: AM Lipski, C Pino, FR Haselton, I-W. Chen and VP Shastri "The effect of silica nanoparticle-modified surfaces on cell morphology, cytoskeletal organization and function", Biomaterials, (28), 3836 (2008)) investigate the effect of nanoparticle (NP) assemblies arranged on a flat substrate on cytoskeletal organization, proliferation and metabolic activity on two cell types. To vary roughness without altering chemistry, glass substrates were coated with monodispersed silica nanoparticles of 50, 100 and 300 nm in diameter. The impact of surface roughness at the nanoscale on cell morphology was studied by quantifying cell spreading, shape, cytoskeletal F-actin alignment, and recruitment of focal adhesion complexes (FAC) using image analysis. In the two cell types tested, surface roughness introduced by nanoparticles had cell type specific effects on cell morphology and metabolism. Interestingly, for both cell types surface roughness promoted the formation of long, thick F-actin fibers, which aligned with the long axis of each cell. Their finding that nanoroughness, as imparted by nanoparticle assemblies, effects cellular processes in a cell specific manner, can have far reaching consequences on the development of "smart" biomaterials especially for directing stem cell differentiation.

[0005] Pennisi et al. (in: Pennisi CP, Dolatshahi-Pirouz A, Foss M, Chevallier J, Fink T, Zachar V, Besenbacher F, Yoshida K. Nanoscale topography reduces fibroblast growth, focal adhesion size and migration-related gene expression on platinum surfaces. Colloids Surf B Biointerfaces. 2011 Jul 1;85(2):189-97. Epub 2011 Feb 26) describes an investigation of the responses of primary human fibroblasts to platinum substrates with different levels of surface roughness at the nanoscale. The nanorough surfaces were fabricated by using the glancing angle deposition technique (GLAD). The levels of cellular responses were found to depend on the surface roughness and the size of the nanoscale features. The authors showed that in response to nanotopography cells spread less and have an elongated morphology, displaying signs of actin cytoskeleton impairment and reduced formation of focal adhesion complexes. Although cell growth and adhesion were impaired on the nanorough substrates, cell viability was not affected by topography. To a minor extent the results also indicated that cell migration might be reduced on the nanorough surfaces, since a significantly lower gene expression of migration related genes were found on the roughest surfaces as compared to the flat reference. The authors conclude that that surface nanotopography influences fibroblasts responses on platinum, which may be used to reduce cellular adhesion on platinum implant surfaces such as implantable neural electrodes.

[0006] Seil and Webster (in: Decreased astroglial cell adhesion and proliferation on zinc oxide nanoparticle polyurethane composites. Int J Nanomedicine. Dec 2008; 3(4): 523-531) describe a study on the activity of astroglial cells on ZnO nanoparticle polymer composites. ZnO nanoparticles embedded in polyurethane were analyzed via scanning electron microscopy to evaluate nanoscale surface features of the composites. The surface chemistry was characterized via X-ray photoelectron spectroscopy. Astroglial cell response was evaluated based on cell adhesion and proliferation. Astrocyte adhesion was significantly reduced on ZnO nanoparticle/polyurethane (PU) composites with a weight ratio of 50:50 (PU:ZnO) wt.%, 75:25 (PU:ZnO) wt.%, and 90:10 (PU:ZnO) wt.% in comparison to pure PU. The successful production of ZnO nanoparticle composite scaffolds suitable for decreasing astroglial cell density demonstrated their potential as a nerve guidance channel material.

[0007] WO 2014/116132 discloses a biomaterial for use in promoting neuronal regeneration in the central nervous system, i.e. to address the lack of capacity of injured axons to spontaneously regenerate in the glial scar microenvironment ("nerve repair strategies"). Al-

though the material itself has a roughness of between about 10 nm and about 50 nm, the roughness is not recognized as relevant for the function.

[0008] Glial scar formation around implanted electrodes soon after implantation into the brain leads to dysfunction of these electrodes. The formation of glial scars around implantable brain electrodes is the dominant contributor to electrode failure. Discovering strategies to inhibit glial scar formation around brain implants is critical for long term electrode function and would thus lead to improvement of treating patients with neurological disorders such as epilepsy or Parkinson's disease.

[0009] Amongst other components, the central nervous system (CNS) is also comprised of extracellular matrix macromolecules and glia support cells, and the contribution of the physical attributes of these components in the maintenance and regulation of neuronal function is not well understood. These components possess well-defined topography.

[0010] In the context of neuronal development and neurophysiology, astrocytes have an established role in maintaining neuronal function. They form a vast network that provides the physical and biochemical matrix over which neurons thrive and function (see, for example, Theodosis D, Poulain D, Oliet S (2008) Activity-dependent structural and functional plasticity of astrocyte-neuron interactions. Physiol Rev: 983-1008. Wade JJ, McDaid LJ, Harkin J, Crunelli V, Kelso J a S (2011) Bidirectional coupling between astrocytes and neurons mediates learning and dynamic coordination in the brain: a multiple modeling approach. PLoS One 6: e29445).

[0011] The plasticity found in the brain can be attributed in part to the morphological changes that occur in astrocyte processes that can alter not only the geometry of the neuronal environment but also induce dynamic changes in astrocyte-neuron interactions impacting neurotransmission, signal gradients and the relationship between synapses. Interestingly, the changes to the neuronal environment induced by astrocytes involve extracellular matrix (ECM) molecules such as proteoglycans (PGs), postulating a significant role for topography in neural development.

[0012] A glioma is a type of tumor that starts in the brain or spine. It is called a glioma because it arises from glial cells, such as astrocytes. Gliomas make up about 30% of all brain and central nervous system tumors and 80% of all malignant brain tumors. Glioblastoma multiforme is a malignant astrocytoma and the most common primary brain tumor among adults.

[0013] Alzheimer's disease is characterized by loss of neuronal function in the central nervous system (CNS). This loss of function occurs predominantly around senile plaques, which mainly consist of amyloid-beta deposits. The exact mechanism by which neuronal death and loss of function occur is currently not well understood.

[0014] Currently therapies are focused on dissolving the beta amyloid deposits and this approach has not been very successful. One approach is to use cholera toxin-B covalently linked to myelin basic protein . Therapies based on anti- amyloid beta plaque antibodies (e.g. Bapineuzumab) jointly developed by Johnson & Johnson and Pfizer have failed in Phase III clinicals. Recently in July of 2014, another beta amyloid plaque targeted antibody (Crenezumab) developed by Roche/Genentech failed to meet its phase II objectives. Thus, there is real need for developing new targets for preventing or reversing loss of neuronal function due to Alzheimer's.

[0015] Satoh et al. (in: Satoh K, Hata M, Takahara S, Tsuzaki H, Yokota H, Akatsu H, Yamamoto T, Kosaka K, Yamada T.A novel membrane protein, encoded by the gene covering KIAA0233, is transcriptionally induced in senile plaque-associated astrocytes. Brain Res. 2006 Sep 7;1108(1):19-27. Epub 2006 Jul 18) in an effort to identify astrocyte-derived molecules that may be intimately associated with progression of AD, identified a novel Abeta-induced rat gene, designated Mib, whose human counterpart covers KIAA0233. In AD brains, Mib is expressed in activated astrocytes associated with senile plaques, but not expressed in neurons around lesions. From these observations, Mib appears to be a novel Amyloid-beta-responsive gene that may play a role in astrocyte inflammatory activation around senile plaques in the AD brain.

[0016] In order to solve the above objects, the present inventors have developed biomaterial surfaces with properties that interfere with the organization of astroglia and fibroblasts, which is necessary for the formation of, for example, a glial scar.

[0017] Thus, in a first aspect of the present invention, the object of the present invention is solved by a neural implant comprising a biomaterial having an outer surface with a stochastic nanoroughness (Rq) of between 25 and 40 nm, preferably of between 32 nm +/- 5 nm, and most preferred of about 32 nm for use in the prevention of glial scar formation

[0018] Disclosed are biomaterial surfaces, either as the surface as such and/or as coatings, with specific topographies found to alter astrocyte phenotype. The surface or coating generates a nanotopography with a specific roughness on the implant surface and is thereby able to prevent problems common with current implants, such as, for example, glial scar formation around the implant in vitro and/or vivo.

[0019] US 2007-0038307 describes nanomaterials for neural and orthopedic prostheses. Composite carbon nanofibers enhance neuronal growth and minimize glial scar tissue formation. Methods and compositions to promote neuronal growth and minimize scar tissue formation during prolonged monitoring and treatment of neural tissue are disclosed. Composite polyurethane carbon nanofiber is a suitable material for neural implant. Composite carbon nanomaterials decrease adhesion of astrocytes and fibroblasts.

[0020] The neural implant can be made out of any of a variety of materials known to be suitable for serving as (part of) a neural implant, preferably as described herein.

Preferred is the neural implant according to the present invention, wherein said biomaterial is selected from platinum, synthetic polymers, for example poly(organo)siloxanes, antimicrobial polymers, materials impregnated/coated with carbon nanotubes (CNTs) and/or graphene, polypyrrole (PPy), poly(3,4-ethylene dioxythiophene) (PEDOT), polyterthiophene (PTTh), cyclotene®, and parylene C.

[0021] Further preferred is a neural implant for use according to the present invention, wherein said implant comprises a component selected from a polymer wire, a nanotube, an array of micro-sized posts or pillars, carbon fibers, and composite carbon nanofibers.

[0022] A wide variety of biomaterials are used in neural implants for the central nervous system (CNS): drugs or gene carriers for treatment of neurological disorders and brain tumors, scaffolds for promoting tissue regeneration, neural electrodes for restoration of lost neurological functions or shunt systems for hydrocephalus. The biomaterials used in the CNS include silicone, lipids, natural polymers and synthetic polymers in various forms based on their applications. Some applications, such as neural electrodes or CNS shunts, require the biomaterials to remain functional indefinitely. Other applications, such as drug carriers or tissue scaffolds, require the biomaterials to degrade after their function is fulfilled. For a review regarding biomaterials that can be used in the context of the present invention, see, for example, Zhong Y and Bellamkonda RV (Biomaterials for the central nervous system. J R Soc Interface. 2008 Sep 6;5(26):957-75).

[0023] Usually, neural implants, such as electrodes for brain implantation, are made out of polymers, metals or a combination of both. Material coatings for these electrodes are not widely used. The surprising advantage of the present invention is the creation of nanotopography on implant surfaces which allows for a control of the behavior of surrounding cells (especially astrocytes which are a main contributor in, for example, glial scar formation).

[0024] Tissue fibrosis, or scar formation, is a common response to damage in most organs of the body. The central nervous system (CNS) is special in that fibrogenic cells are restricted to vascular and meningeal niches. However, disruption of the blood-brain barrier and inflammation can unleash stromal cells and trigger scar formation. Astroglia segregate from the inflammatory lesion core, and the so-called "glial scar" composed of hypertrophic astrocytes seals off the intact neural tissue from damage. In the lesion core, a second type of "fibrotic scar" develops, which is sensitive to inflammatory mediators. The fibrotic scar represents a major barrier to CNS regeneration. Preventing of fibrosis may therefore prove to be a valuable therapeutic strategy for neurological disorders such as stroke, spinal cord injury and multiple sclerosis (see Fernández-Klett F, Priller J. The fibrotic scar in neurological disorders. Brain Pathol. 2014 Jul;24(4):404-13).

[0025] By inhibiting glial scar formation around implantable neural, e.g. brain, electrodes for use according to the present invention, it is possible to use these devices for long term treatments and therapies, which is currently not possible.

[0026] Preferred is a neural implant for use according to the present invention, wherein said implant is permanent or non-permanent and is preferably selected from a measuring and/or stimulating electrode, such as flexible nanoelectrodes, a pacemaker, and a drug delivery device.

[0027] As described herein, the neural implant for use according to the present invention can be used, at least in part, as a drug delivery device. Thus, further preferred is a neural implant for use according to the present invention, wherein said biomaterial further comprises an active substance, which can be preferably selected from a pharmaceutically active drug, an antibiotic, a cytotoxic substance, an anti-inflammatory substance, a polypeptide, a polysaccharide, NGF, and collagen or other neurotropic and neuroprotective agents, such as, for example, BDNF.

[0028] Asplund et al. (Asplund M, Boehler C, Stieglitz T. Anti-inflammatory polymer electrodes for glial scar treatment: bringing the conceptual idea to future results. Front Neuroeng. 2014 May 13;7:9) describe polymer electrodes that could also be useful as implants in the context of the present invention.

[0029] The inventors envisage the invention to lead to an improved therapeutic use of brain electrodes and other neural (e.g. brain) implants. Especially, the use in deep brain stimulation of Parkinson's disease patients is disclosed.

[0030] Disclosed is a method for producing the neural implant for use according to the present invention as described herein, comprising the step of providing a prefabricated neural implant device with a biomaterial having an outer surface with a stochastic nanoroughness (Rq) of between 25 and 40 nm, preferably of between 32 nm +/- 5 nm, and most preferred of about 32 nm. In the context of the present application, "about" shall mean +/- 10 percent of a given value.

[0031] Preferred is a method as disclosed, wherein said prefabricated neural implant device at least partially consists out of said biomaterial, or wherein said biomaterial is applied as a coating to said prefabricated neural implant device. The method can also comprise the prefabrication of the neural implant, including providing of the nanoroughness directly or indirectly (i.e. during production or as a separate production step) to the implant. Additionally/alternatively, in a preferred method as disclosed, stochastic nanoroughness (Rq) is applied to said biomaterial using a suitable method known to the person of skill, preferably selected from polishing, machining, surface treatment, coating, cathodic polarization, acid etching, rolling, atmospheric plasma, laser treatment, and casting.

[0032] The present inventors envisage the invention to lead to an improved therapeutic use of brain electrodes

and other brain implants.

[0033] Preferably, the method also comprises a method of producing said implant as described herein, before implanting it.

[0034] A mammal in the context of the present invention preferably is selected from a mouse, rat, monkey, goat, sheep, cat, dog, horse, rabbit, pig, and human.

[0035] The finding that regions of amyloid plaque build-up in Alzheimer's involve changes to tissue nanoroughness provides a link between nanoscale physical cues and loss of function in neurons.

[0036] In sum, the key findings of the present invention provide evidence for the hitherto unexplored role for ECM and glial cell associated changes to stochastic nanoroughness in neurodevelopment and neuropathologies.

[0037] The present invention will now be described further in the following examples with reference to the accompanying figures, nevertheless, without being limited thereto.

[0038] In the Figures:

Figure 1 shows a panel of the formation of glial scar tissue in vitro on a smooth glass surface (top panel; Rq = 3.5 nm). In comparison, no glial scar tissue is formed on surfaces with a modified topography (bottom panel; Rq = 32nm). Rq is the root mean square roughness.

Figure 2 shows (left) the relative amount of glial scar tissue formed in vitro around polymer wires (grey bar) or coated polymer wires with an altered surface topography (black bar). The right figure shows the size of glial scar tissue formed in vitro after re-plating onto plain glass which is a smooth surface (black line) or surfaces with a modified topography, Rq 32 nm (grey line).

Figure 3 shows the morphological and functional traits in PC-12 cells on nanorough substrates: (a) Atomic force microscopy (AFM) of silica nanoparticle (SNP) modified substrates with the corresponding surface roughness Rq . (b) Morphology of PC-12 cells on Rq = 3.5nm, Rq = 32nm and Rq = 80 nm visualized by staining for F-actin. Impact of nanoroughness on PC-12 polarization as assessed by determining: (c) number of neurites per cell and (d) neurite length. (e) Influence of nanoroughness on acetylcholinesterase (AChE) activity. Calcium sensitive FURA-2 imaging of differentiated PC-12 cells on smooth glass substrates and surfaces with an Rq of 32 nm: (f) change in intracellular calcium levels as assessed by FURA-2 intensity, (g) rate of depolarization as determined by the slope of the depolarization portion of the curve (immediately after addition of KCl). Statistical significance: * $p<0.05$; ** $p<0.01$; *** $p<0.001$.

Figure 4 shows that the morphology and function of rat hippocampal neurons and astrocytes are influenced by substrate roughnesses: Neuron-astrocyte interaction on (a) smooth glass substrate, (b) on substrate of Rq = 32nm. Astrocytes were visualized using antibody against GFAP (dark gray) and neurons were visualized using antibody against MAP-2 (light gray). Quantification of neuron-astrocyte association in: (c) short-term cultures (5 days), and (d) long-term cultures (6 weeks). Calcium sensitive FURA-2 imaging in hippocampal neurons on smooth glass substrates and surfaces with Rq of 32 nm: (e) change in intracellular calcium level as assessed by FURA-2 intensity, (f) rate of depolarization as determined by the slope of the depolarization portion of the curve (immediately after addition of KCl). Statistical significance: *** $p<0.001$.

Figure 5 shows that piezo-1 is necessary for sensing nanotopography: (a) Representative scanning electron micrograph of PC-12 cells grown on nanorough surface (shown Rq = 40nm). PC-12 stained using anti-FAM38A, an antibody for Piezo-1 mechanosensitive ion channel on Rq = 3.5nm (b) and Rq = 32nm (c). On smooth surfaces, FAM38A staining is pronounced at neurite branch points (denoted by circles) (b), while on nanorough surfaces FAM38A staining is uniform along all neurite processes (c). Rat dorsal root ganglia morphology (d, e) and function (f, g) on glass and Rq of 32nm. Inhibition of FAM38A with GsMTx4 (5μM) results in decoupling of hippocampal neurons from astrocytes on smooth glass substrates (h, i). The FURA-2 intensity profile (j), and rate of calcium influx (k) in hippocampal neurons upon depolarization with KCl on smooth glass substrate and Rq = 32nm is identical upon inhibition of FAM38A. Statistical significance: *** $p<0.001$.

Figure 6 shows that nanoroughness alters physical attributes of astrocytes: Dependency of astrocyte form factor on substrate nanoroughness: (a) Decrease in form factor on 32 nm Rq surfaces is consistent with a more motile phenotype (inset). Morphological changes to astrocyte cell surface on nanorough surfaces: AFM images of astrocytes grown on glass (b) and on Rq=32nm (c) and the corresponding transverse line scans, and changes to topography of astrocyte surface on 32 nm surfaces (d). Shaded areas show representative areas for Rq calculations. Amyloid-beta plaques are associated with topographical changes to brain tissue: Paraffin embedded human brain slices stained with Bielschowsky's silver stain (e): Left image; healthy human (AD-), Right image; patient diagnosed with Alzheimer's (AD+): revealing amyloid β plaques indicated by yellow arrowheads. Bottom panel; tapping mode AFM scans (10μm x 10 μm) of one of the representative areas (top), higher magnification (2 μm x 2μm) scan of the same area (bottom), and transverse

views of the corresponding 2 μm x 2μm image above. (f) Histograms of Rq values of healthy brain tissue, and amyloid-B plaques in Alzheimer's patients showing a general shift of tissue roughness to higher Rq 's and an increased heterogeneity in roughness in AD+ brain slices. Rq values were calculated using a 700 nm x700 nm scan area.

EXAMPLES

Example 1

[0039] The properties of the inventive biomaterial surface for use were tested and verified in a clinically relevant experimental model. In the in vitro model of glial scarring, polymer wires with the surface coating were able to inhibit glial scar formation. Moreover, already (in vitro) formed glial scar tissue decomposed when exposed to a specific regimen of nanotopography as it is used for the coating. Polymer wires with surface coating were implanted into Agarose gels with an almost similar consistency as brain tissue, and the coating was shown to be stable after this implantation (see Figures 1 and 2).

[0040] The surfaces of the materials can be characterized for morphology and roughness using scanning electron microscopy (SEM).

Example 2

Nanotopography modulates PC-12 cell polarity and enhances function

[0041] Since macromolecules are in a state of high entropy, and entropy is a statistical measure of randomness, the roughness presented by macromolecules is expected to be stochastic (random). The inventors simulated random ECM nanoroughness using an assembly of monodispersed silica colloids of increasing size (Lipski AM, Pino CJ, Haselton FR, Chen I-W, Shastri VP (2008) The effect of silica nanoparticle-modified surfaces on cell morphology, cytoskeletal organization and function. Biomaterials 29:3836-46, Lipski a. M et al. (2007) Nanoscale Engineering of Biomaterial Surfaces. Adv Mater 19:553-557) (Figure 3a). The roughness in this system scales logarithmically with nanoparticles radius and can recapitulate topography from the level of receptor clusters to ECM features (Shastri VP (2009) In vivo engineering of tissues: Biological considerations, challenges, strategies, and future directions. Adv Mater 21:3246-54), and further allows the production of surfaces with stochastic nanoroughness. In contrast, surfaces consisting of periodic groves and ridges that have been extensively studied present deterministic roughness.

[0042] As a first step, the inventors investigated the ability of PC-12 cells (Greene L, Tischler S (1976) Establishment of a noradrenergic clonal line of rat adrenal pheochromocytoma cells which respond to nerve growth factor. Proc Natl Acad Sci U S A 73:2424-8), a well-established model system for studying neuronal differentiation, to perceive stochastic nanoroughness and analyzed changes to their morphology and function.

[0043] PC12 cells are indeed able to perceive the underlying nanoroughness (in an NGF- and collagen-dependent manner) and showed an increased differentiation and associated functional traits on a specific Rq of about 32 nm as evident from a highly polarized cell morphology (Figure 3b, middle panel) and associated changes such as fewer and longer neurite outgrowths (Figure 3c and 3d) compared to glass, which is considered a smooth substrate (Rq approx. 3.5 nm, Figure 3b, left panel). Beyond this optimal substrate roughness, cells were more prone to clumping (Figure 3b, right panel). If the slides or culture substrates is not coated with collagen, then the PC-12 cells cannot sense the roughness, and also they need NGF in order to express neurites which are the sensing elements for sensing the nanotopography. For growing neuronal cells, in general one has to coat the substrate with either collagen polylysine or other polycation, such as poly-L-ornithine. Nevertheless, this coating does not affect the roughness and/or Rq values.

[0044] One measure of the functional state of a neuron is the activity of acetylcholinesterase (AChE) as this is necessary for synaptic communication. Interestingly, AChE levels also peaked in PC-12 cells on 32 nm Rq surfaces (Figure 3e), which also coincided with an accelerated and elevated calcium response to depolarization (Figures 3f and 3g).

Nanotopography mediates hippocampal neuron-astrocyte interaction

[0045] The inventors then posed the following question: can neuronal cells in general perceive nanoroughness and, if so, does it have a role in defining their interaction and function? Hippocampal neurons are responsible for memory formation. Loss of their function and death has been linked to neuropathologies, such as Parkinson's and Alzheimer's disease.

[0046] The inventors therefore evaluated the response of mixed primary cultures of rat hippocampal neurons and astrocytes to the different roughness regimes. Surprisingly, primary hippocampal neurons also responded to roughness in a manner similar to dopaminergic PC-12, and exhibited prominent, axon like polarized structures on exactly the same Rq of 32nm.

[0047] An also remarkable finding was that nanoroughness appeared to modulate the relationship, and dependency of neurons on astrocytes. It is well established that neurons require astrocytes for survival (Cui W, Allen ND, Skynner M, Gusterson B, Clark a J (2001) Inducible ablation of astrocytes shows that these cells are required for neuronal survival in the adult brain. Glia 34:272-82), and indeed, on surfaces with an Rq above and below 32 nm, neurons were predominantly found associated with astrocytes (Figures 4a and 4c). However, on Rq of approx. 32 nm, neurons were dissociated from astrocytes

(Figures 4b and 4c) and continued to survive independently even up to 6 weeks (Figure 4d). After 5 days, the percent neurons that were associated with astrocytes on the 32 nm Rq surface was around 15%, which was 1.5 - 2 fold lower than those on other Rq's, which ranged from 20 - 40 %, and 6 fold lower than that on the smooth glass substrate (Figure 4c). That is, in comparison to the other Rq's, over twice as many neurons on 32 nm Rq surface were surviving independently of astrocytes. At 6 weeks however, the percent of neurons that were surviving independently of astrocytes on the 32 nm Rq was over 6 fold greater in comparison to the other Rq's. While over 90% of neurons were associated with astrocytes on other roughnesses, only 15% of neurons were associated with astrocytes on 32 nm Rq (Figure 4d). Remarkably, hippocampal neurons on 32 nm Rq surfaces in spite of being dissociated from astrocytes showed an order of magnitude faster and stronger increase in intracellular calcium levels following membrane depolarization in comparison to those on smooth surfaces (Figures 4e and 4f). Thus, there seemed to be a favorable Rq of around 32 nm at which both PC-12 and hippocampal neurons appeared to be more functional.

Mechanosensing ion channel - Piezo-1 is responsible for the sensing of nanoscale physical cues by neurons

[0048] Past studies showed that stochastic nanoroughness altered the organization of focal adhesion complexes in highly migratory preosteoblasts and endothelial cells (AM Lipski, C Pino, FR Haselton, I-W. Chen, and VP Shastri; "The effect of silica nanoparticle-modified surfaces on cell morphology, cytoskeletal organization and function", Biomaterials, (28), 3836 (2008)). Since neurons have limited migratory capacity (Fricker R a et al. (1999) Site-specific migration and neuronal differentiation of human neural progenitor cells after transplantation in the adult rat brain. J Neurosci 19:5990-6005), a critical open question was how neurons perceive nanoroughness. Scanning electron micrographs revealed that the neurites indeed make intimate contact with the underlying topography (Figure 5a). Such intimate contact between the neurites and the surface ought to manifest itself as changes in membrane tension. Since the conformation and distribution of mechanosensitive ion channels is altered in response to changes in membrane tension and curvature (Nilius B (2010) Pressing and squeezing with Piezos. EMBO Rep 11:902-3), the inventors investigated the expression pattern of FAM38A, an integrin-activated transmembrane protein, which is part of the mechanosensitive ion channel Piezo-1 (Coste B et al. (2010) Piezol and Piezo2 are essential components of distinct mechanically activated cation channels. Science 330:55-60). Piezo-1 is expressed by CNS neurons and not by sensory neurons like dorsal root ganglia (DRG) (Roudaut Y et al. (2012) Touch sense: functional organization and molecular determinants of mechanosensitive receptors. Channels 6:234-45).

[0049] It was observed that, while FAM38A expression in PC-12 cells on glass was predominantly localized at neurite branch-points which would be a region of high cytoskeletal tension (Figure 5b), in contrast, a more uniform distribution of FAM38A could be seen on the optimal Rq of 32 nm, suggesting a dramatic change to the mechanical environment of the neurite as they perceive the nanoroughness (Figure 5c). Since FAM38A expression level was not altered, and PC-12 during differentiation did not show any changes in attachment force or motility in response to nanoroughness, the observed changes to Piezo-1 expression pattern can be linked to the underlying nanotopography.

[0050] The role of Piezo-1 in sensing topography is further bolstered by the findings that DRGs, which lack this mechanosensitive channel, but possess Piezo-2 instead, do not show any morphological changes on nanoroughness substrates (Figures 5d and 5e). This is further confirmed by imaging the calcium flux, which showed similar depolarization patterns and rate of calcium influx in DRGs grown on Rq of 3.5 and DRGs grown on Rq of 32 nm (Figures 5f and 5g).

Neuron-astrocyte interactions involve topographical cues provided by astrocytes and Piezo-1

[0051] As indicated above, primary hippocampal neurons require the interaction with astrocytes for their survival (Cui W, Allen ND, Skynner M, Gusterson B, Clark a J (2001) Inducible ablation of astrocytes shows that these cells are required for neuronal survival in the adult brain. Glia 34:272-82). This raised the question as to why do the neurons favor the surface over association with the astrocytes. AFM analysis of the surface of astrocytes associated with neurons led the inventors to the remarkable finding that the roughness of the astrocyte surface was around an Rq of 26 - 28 nm (Figure 6d), and this coincides rather well with the roughness regime on which neurons exhibit decoupling from astrocytes.

[0052] A role of mechanotransduction in maintaining neuron-astrocyte interactions is further supported by the inventors' findings that upon inhibition of Piezo-1 with the toxin GsMTx4 (Delmas P, Hao J, Rodat-Despoix L (2011) Molecular mechanisms of mechanotransduction in mammalian sensory neurons. Nat Rev Neurosci 12:139-53, Bae C, Sachs F, Gottlieb P (2011) The mechanosensitive ion channel Piezol is inhibited by the peptide GsMTx4. Biochemistry 50:6295-6300), neurons decouple from astrocytes even on smooth glass substrates (Figures 5h and 5i) where their normally show strong association (Figures 4a, 4c, and 4d). Furthermore, the increased sensitivity to depolarization that was observed in hippocampal neurons on Rq of 32 nm is lost upon inhibition of Piezo-1 (Figures 5j and 5k). This provides direct evidence for the role of nanotopography is influencing hippocampal neuron-astrocyte interaction and function through mechanotransduction, and a clear role for stretch-activate ion channels in these processes.

Regions of amyloid plaque build-up in Alzheimer's present increased tissue nanoroughness

[0053] The inventors' observation that topography of astrocytes, a support cell for neurons, can dictate the function of the phenotypically unrelated neurons, points to a larger paradigm wherein physical and mechanical information provided by astrocytes and ECM macromolecules play a role not only in neuronal development but also in neuropathologies. There is ample evidence that the loss of memory associated with Alzheimer's disease (AD) is due to the death of hippocampal neurons. PGs like chondroitin sulfate PGS (CSPGs) have been implicated both in neural differentiation and neuropathologies such as Alzheimer's (Galtrey CM, Fawcett JW (2007) The role of chondroitin sulfate proteoglycans in regeneration and plasticity in the central nervous system. Brain Res Rev 54:1-18). CSPGs have been found to co-localize with amyloid-β plaques, and *in vitro* studies have shown that CSPGs can promote amyloid-β fibril assembly a key step in plaque formation. Interestingly, amyloid-β stimulates CSPG production in astrocytes, which has negative effects on neuronal health and synapse formation.

[0054] Thus, the loss of hippocampal neuron function in Alzheimer's seems to be triggered by changes to the topography that the neurons experience. In order to investigate this premise further, the inventors analyzed the topographical characteristics of amyloid-β plaques in the hippocampus of human brain slices using AFM (Figure 6e). The inventors made the compelling observation that while the Rq of healthy brain tissue (AD-) showed a Gaussian distribution with a median centered around 34 nm, the tissue of individuals diagnosed with Alzheimer's (AD+) showed a bimodal distribution of tissue roughness with a pronounced shift in the median towards higher Rq values of 60 nm accompanied by a more heterogeneous Rq pattern (Figure 6f). The emergence of Rq values greater than 80 nm, which is the range of Rq where the inventors observe increased neuronal cell death, is in accordance with published reports that neurons, when exposed to amyloid-β undergo apoptosis (Fraser PE, Lévesque L, McLachlan DR (1994) Alzheimer A beta amyloid forms an inhibitory neuronal substrate. J Neurochem 62:1227-30; Ivins KJ, Thornton PL, Rohn TT, Cotman CW (1999) Neuronal apoptosis induced by beta-amyloid is mediated by caspase-8. Neurobiol Dis 6:440-9). The current observation that astrocyte shape is affected by nanoroughness provides evidence that cell signaling in the neuronal environment may be additionally mediated by ECM-based cues.

[0055] The effects of stochastic nanoroughness on neuronal health seem to manifest itself in two possible scenarios: (1) The changes to tissue roughness affects glial cell behavior which then instigates changes to neuron signaling environment, and/or (2) the changes to generally stationary cells that provide a supportive network for neuronal cells and synapses, migratory and proliferating astrocytes have been observed in glial scarring, an environment with diminish neuronal function (Buffo A, Rolando C, Ceruti S (2010) Astrocytes in the damaged brain: molecular and cellular insights into their reactive response and healing potential. Biochem Pharmacol 79:77-89, Wanner IB et al. (2013) Glial scar borders are formed by newly proliferated, elongated astrocytes that interact to corral inflammatory and fibrotic cells via STAT3-dependent mechanisms after spinal cord injury. J Neurosci 33:12870-86). In the present invention, an altered cellular environment in the form of nanotopography was shown to affect astrocyte biophysical attributes (shape, roughness) so as to alter its interaction with neurons. Strong evidence for the second scenario is derived from a recent study by Satoh et al. (Satoh K et al. (2006) A novel membrane protein, encoded by the gene covering KIAA0233, is transcriptionally induced in senile plaque-associated astrocytes. Brain Res 1108:19-27), showed that hMib (a human ortholog of rodent Piezo-1) is transcriptionally induced in activated astrocytes associated with senile amyloid-β plaques in AD+ human brains. Interestingly, neurons that express hMib show damaged morphology while healthy looking neurons do not express hMib. The ability to sense the changes to astrocyte topography induced by tissue roughness seems to have triggered undesirable changes in hMib+ neurons. Conversely, the inability to sense the mechanical cues provided by the astrocytes seems to play a role in the loss of function in the hMib- neurons. Since healthy neurons are hMib+, loss of this marker seems to additionally play a role in the functional deficiency associated with Alzheimer's.

SEQUENCE LISTING

[0056]

<110> Universitätsklinikum Freiburg

<120> Improved biomaterials for neuronal implants and use of said biomaterials in the diagnosis and therapy of neuronal diseases

<130> U30584EP

<160> 4

<170> PatentIn version 3.5

<210> 1
<211> 19
<212> RNA
<213> Homo sapiens

<400> 1
gcacaaaggc cuccgacuu 19

<210> 2

<211> 19
<212> RNA
<213> Homo sapiens

<400> 2
ggguugaaga uucgggaga 19

<210> 3
<211> 19
<212> RNA
<213> Homo sapiens

<400> 3
cggaagaaug gcagcgcau 19

<210> 4
<211> 19
<212> RNA
<213> Homo sapiens

<400> 4
cagaugaaca guugggcga 19

Claims

1. A neural implant comprising a biomaterial having an outer surface with a stochastic nanoroughness (Rq) of between 25 and 40 nm for use in the prevention of glial scar formation.

2. The neural implant for use according to claim 1, wherein said stochastic nanoroughness (Rq) is between 32 nm +/- 5 nm, such as about 32 nm.

3. The neural implant for use according to claim 1 or 2, wherein said biomaterial is selected from platinum, gold, synthetic polymers, for example poly(organo)siloxanes, antimicrobial polymers, polypyrrole (PPy), poly(3,4-ethylene dioxythiophene) (PEDOT), polyterthiophene (PTTh), poly(pyrrole) and its derivatives, cyclotene®, and parylene C.

4. The neural implant for use according to any one of claims 1 to 3, wherein said biomaterial further comprises an active substance selected from a pharmaceutically active drug, an antibiotic, a cytotoxic substance, an anti-inflammatory substance, a polypeptide, NGF, BNDF, and collagen.

5. The neural implant for use according to any one of claims 1 to 4, wherein said implant comprises a component selected from a polymer wire, a nanotube, an array of micro-sized posts or pillars, carbon fibers, and composite carbon nanofibers.

6. The neural implant for use according to any one of claims 1 to 5, wherein said implant is permanent or non-permanent and is preferably selected from a measuring and/or stimulating electrode, such as flexible nanoelectrodes, a pacemaker, and a drug delivery device.

7. The neural implant for use according to any one of claims 1 to 6, wherein said glial scar formation is prevented in a neurological disorder selected from epilepsy, Parkinson's disease, Alzheimer's disease, and brain cancer.

Patentansprüche

1. Neuronales Implantat umfassend ein Biomaterial mit einer äußeren Oberfläche mit einer stochastischen Nanorauheit (Rq) zwischen 25 und 40 nm, zur Verwendung in der Verhinderung der Narbenbildung in Gliazellen.

2. Neuronales Implantat zur Verwendung nach Anspruch 1, wobei die stochastische Nanorauheit (Rq) zwischen 32 nm +/- 5 nm, wie beispielsweise bei ungefähr 32 nm, liegt.

3. Neuronales Implantat zur Verwendung nach Anspruch 1 oder 2, wobei das Biomaterial ausgewählt ist aus Platin, Gold, synthetischen Polymeren, zum Beispiel Poly(organo)siloxanen, antimikrobiellen Polymeren, Polypyrrol (PPy), Poly(3,4-ethylendioxythiophen) (PEDOT), Polyterthiophen (PTTh), Poly(pyrrol) und seinen Derivaten, Cyclotene® und Parylen C.

4. Neuronales Implantat zur Verwendung nach einem der Ansprüche 1 bis 3, wobei das Biomaterial ferner einen Wirkstoff umfasst, ausgewählt aus einem pharmazeutisch aktiven Wirkstoff, einem Antibiotikum, einer zytotoxischen Substanz, einer entzündungshemmenden Substanz, einem Polypeptid, NGF, BNDF und Kollagen.

5. Neuronales Implantat zur Verwendung nach einem der Ansprüche 1 bis 4, wobei das Implantat eine Komponente umfasst, die ausgewählt ist aus einem Polymerdraht, einem Nanoröhrchen, einer Anordnung von mikroskopisch kleinen Säulen oder Stützen, Kohlenstofffasern und Kohlenstoff-Nanofasern aus Verbundwerkstoffen.

6. Neuronales Implantat zur Verwendung nach einem der Ansprüche 1 bis 5, wobei das Implantat permanent oder nicht permanent ist und vorzugsweise ausgewählt ist aus einer Mess- und/oder Stimulationselektrode, wie beispielsweise flexiblen Nanoelektroden, einem Schrittmacher und einer Vorrichtung zur Abgabe von Wirkstoffen.

7. Neuronales Implantat zur Verwendung nach einem der Ansprüche 1 bis 6, wobei die Narbenbildung in Gliazellen bei einer neurologischen Störung ausgewählt aus Epilepsie, Parkinson-Krankheit, Alzheimer-Krankheit und Hirnkrebs verhindert wird.

Revendications

1. Implant neural comprenant un biomatériau ayant une surface extérieure avec une nano-rugosité stochastique (Rq) comprise entre 25 et 40 nm, pour une utilisation dans la prévention de la formation de cicatrices gliales.

2. Implant neural pour une utilisation selon la revendication 1, dans lequel ladite nano-rugosité stochastique (Rq) est comprise entre 32 nm ± 5 mm, telle qu'environ 32 nm.

3. Implant neural pour une utilisation selon la revendication 1 ou 2, dans lequel ledit biomatériau est choisi parmi le platine, l'or, les polymères synthétiques, par exemple les poly(organo)siloxanes, les polymères antimicrobiens, le polypyrrole (PPy), le poly(3,4-éthylène-dioxythiophène) (PEDOT), le polyterthiophène (PTTh), le poly(pyrrole) et ses dérivés, le Cyclotene® et le parylène C.

4. Implant neural pour une utilisation selon l'une quelconque des revendications 1 à 3, dans lequel ledit biomatériau comprend en outre une substance active choisie parmi un médicament ayant une activité pharmaceutique, un antibiotique, une substance cytotoxique, une substance anti-inflammatoire, un polypeptide, le NGF, le BNDF, et le collagène.

5. Implant neural pour une utilisation selon l'une quelconque des revendications 1 à 4, lequel implant comprend un composant choisi parmi un fil polymère, un nanotube, un réseau de poutres ou piliers de taille micrométrique, les fibres de carbone, et les nanofibres de carbone composites.

6. Implant neural pour une utilisation selon l'une quelconque des revendications 1 à 5, lequel implant est permanent ou non permanent et est de préférence choisi parmi une électrode de mesure et/ou de stimulation, telle que des nanoélectrodes flexibles, un stimulateur, et un dispositif de délivrance de médicament.

7. Implant neural pour une utilisation selon l'une quelconque des revendications 1 à 6, dans lequel ladite formation de cicatrices gliales est empêchée dans un trouble neurologique choisi parmi l'épilepsie, la maladie de Parkinson, la maladie d'Alzheimer, et un cancer du cerveau.

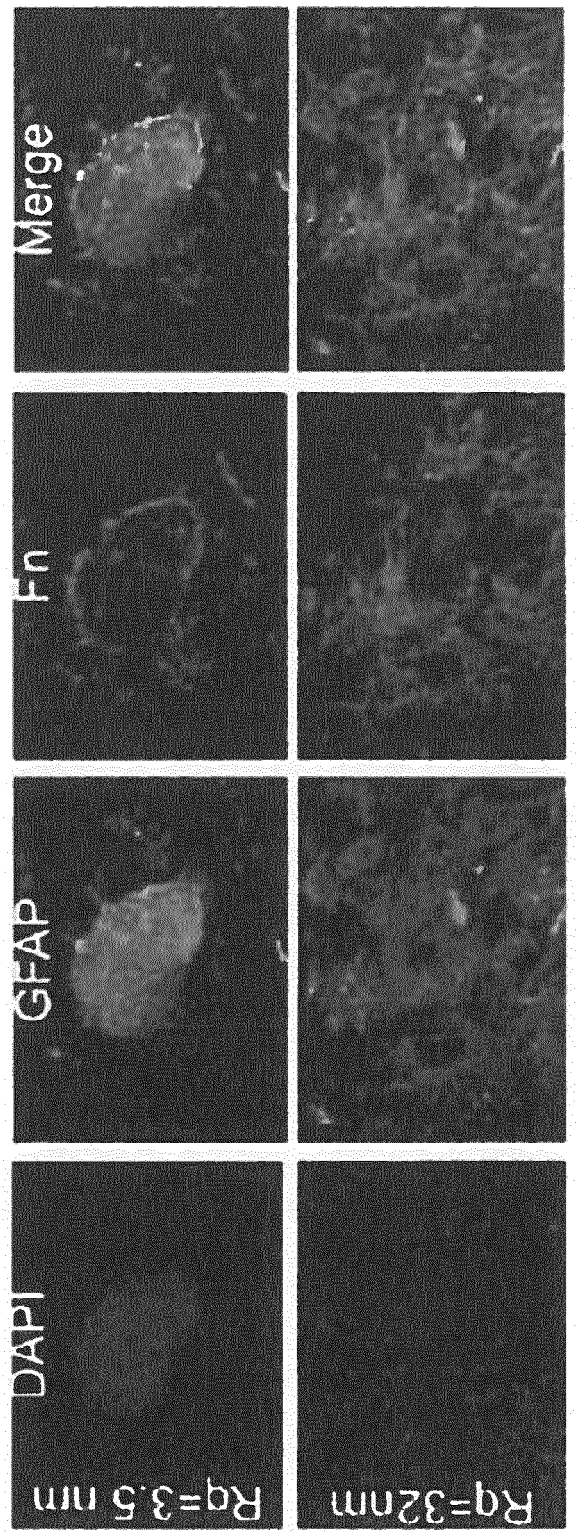

Figure 1

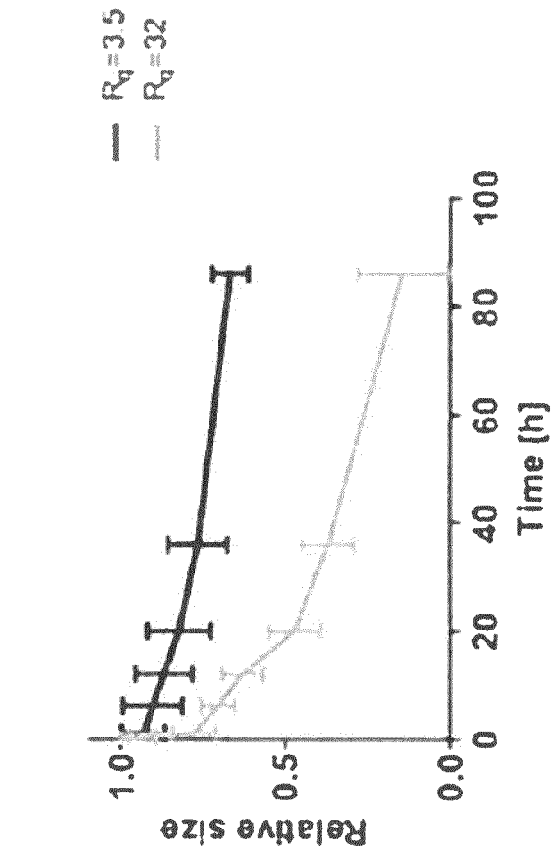
R_q=3.5
R_q=32
Relative size
1.0
0.5
0.0
0
20
40
60
80
100
Time [h]

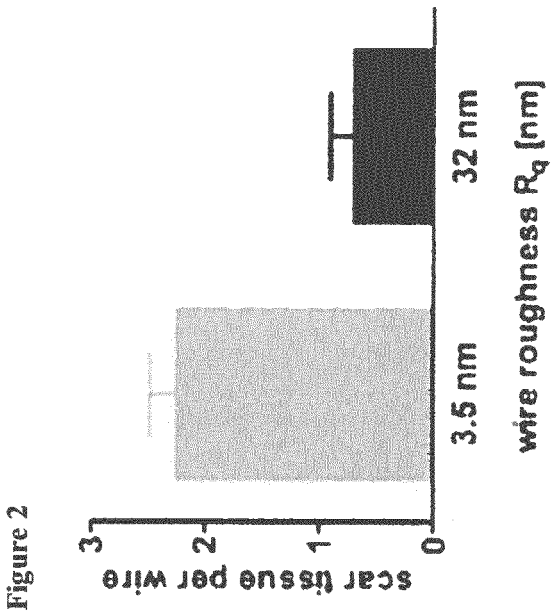
scar tissue per wire
3
2
1
0
3.5 nm
32 nm
wire roughness R_q [nm]

Figure 2

Figure 3

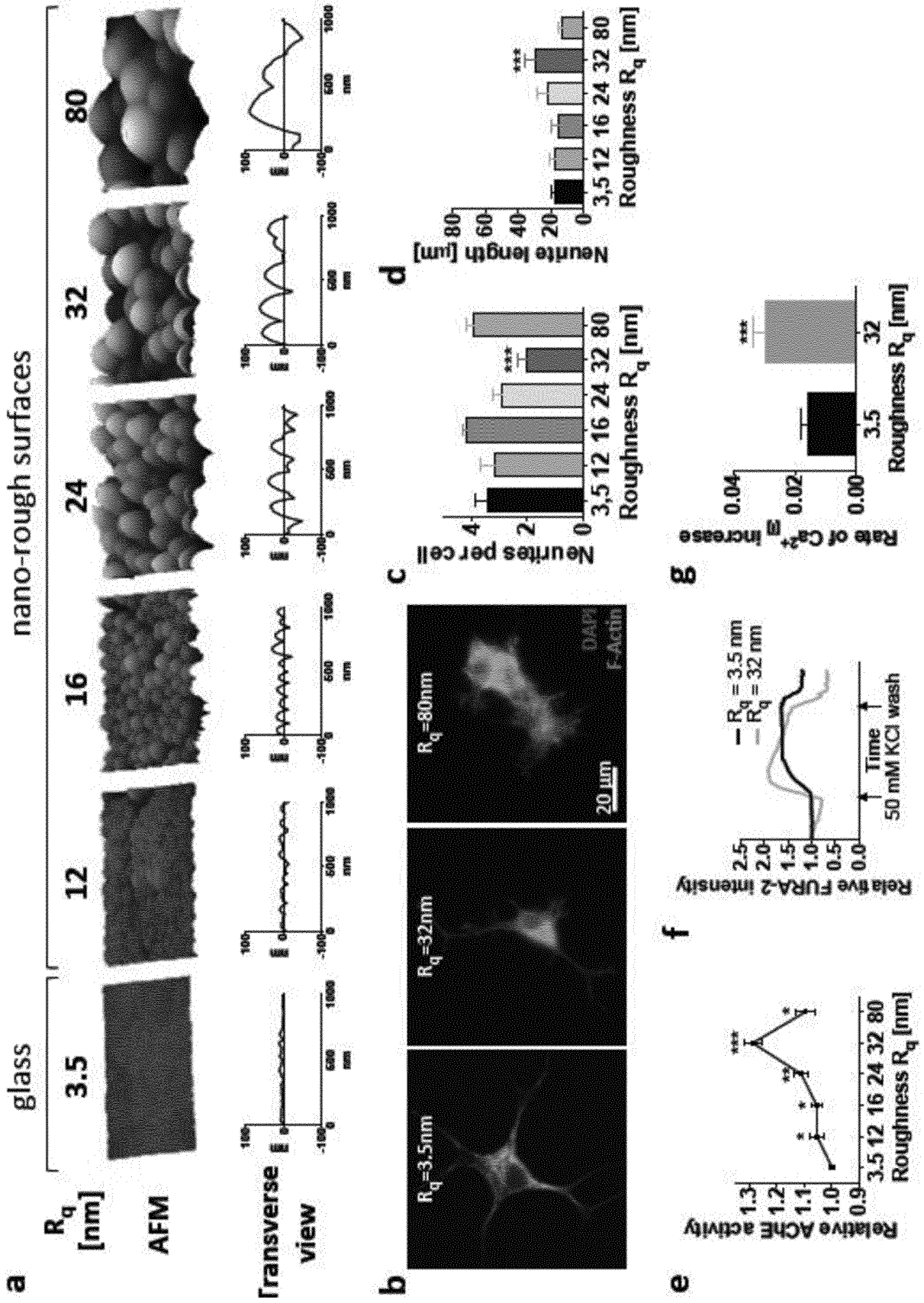
a
glass
nano-rough surfaces
R_q [nm]
3.5
12
16
24
32
80
AFM
Transverse view
b
R_q=3.5nm
R_q=32nm
R_q=80nm
DAPI
F-Actin
20 µm
c
Neurites per cell
Roughness R_q [nm]
d
Neurite length [µm]
Roughness R_q [nm]
e
Relative AChE activity
Roughness R_q [nm]
f
Relative FURA-2 intensity
R_q = 3.5 nm
R_q = 32 nm
Time
50 mM KCl wash
g
Rate of Ca^{2+} increase
Roughness R_q [nm]

Figure 4

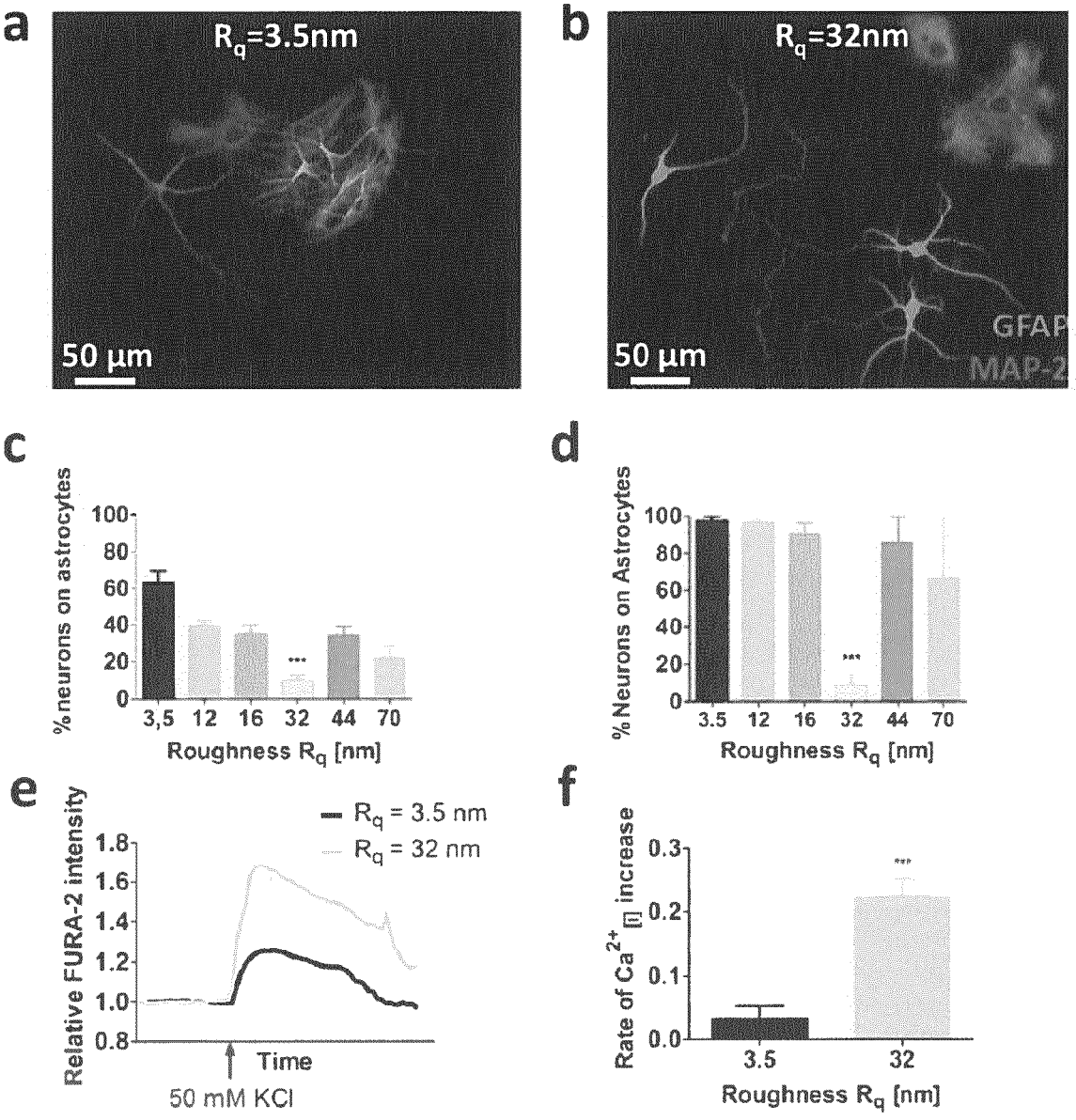
a
Rq=3.5nm
50 µm
b
Rq=32nm
50 µm
GFAP
MAP-2
c
% neurons on astrocytes
100
80
60
40
20
0
***
3,5 12 16 32 44 70
Roughness Rq [nm]
d
% Neurons on Astrocytes
100
80
60
40
20
0
***
3.5 12 16 32 44 70
Roughness Rq [nm]
e
Relative FURA-2 intensity
Rq = 3.5 nm
Rq = 32 nm
1.8
1.6
1.4
1.2
1.0
0.8
Time
50 mM KCl
f
Rate of Ca2+ [i] increase
0.3
0.2
0.1
0.0
***
3.5
32
Roughness Rq [nm]

Figure 5

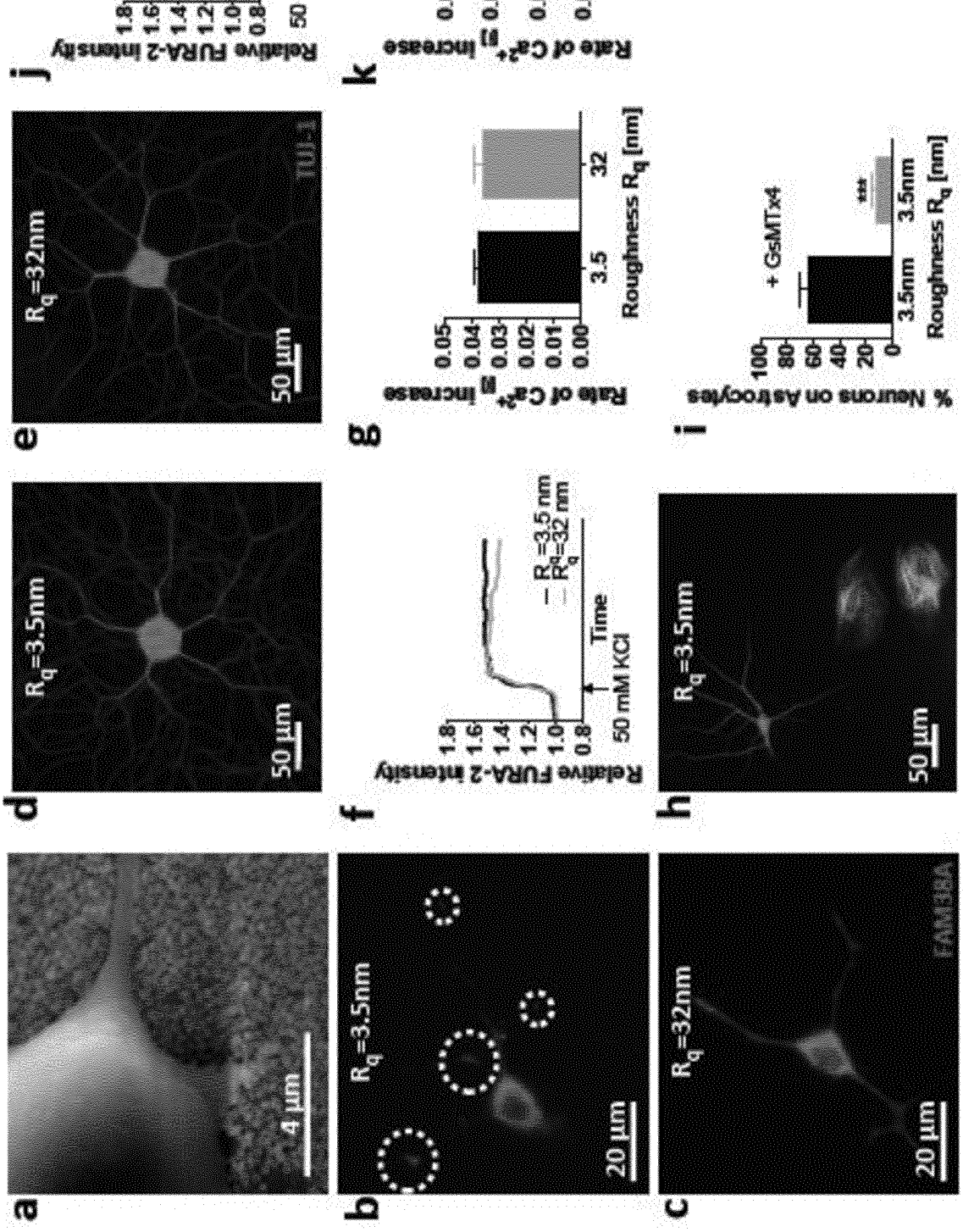
a
4 µm
b
R_q=3.5nm
20 µm
c
R_q=32nm
20 µm
FAM18A
d
R_q=3.5nm
50 µm
e
R_q=32nm
50 µm
TUJ-1
f
Relative FURA-2 intensity
1.8
1.6
1.4
1.2
1.0
0.8
R_q=3.5 nm
R_q=32 nm
Time
50 mM KCl
g
Rate of Ca^{2+}_{in} increase
0.05
0.04
0.03
0.02
0.01
0.00
3.5
32
Roughness R_q [nm]
h
R_q=3.5nm
50 µm
i
% Neurons on Astrocytes
100
80
60
40
20
0
+ GsMTx4
###
3.5nm
3.5nm
Roughness R_q [nm]
j
Relative FURA-2 intensity
1.8
1.6
1.4
1.2
1.0
0.8
+ GsMTx4
R_q=3.5nm
R_q=32nm
Time
50 mM KCl
k
Rate of Ca^{2+}_{in} increase
0.06
0.04
0.02
0.00
+ GsMTx4
3.5
32
Roughness R_q [nm]

Figure 6

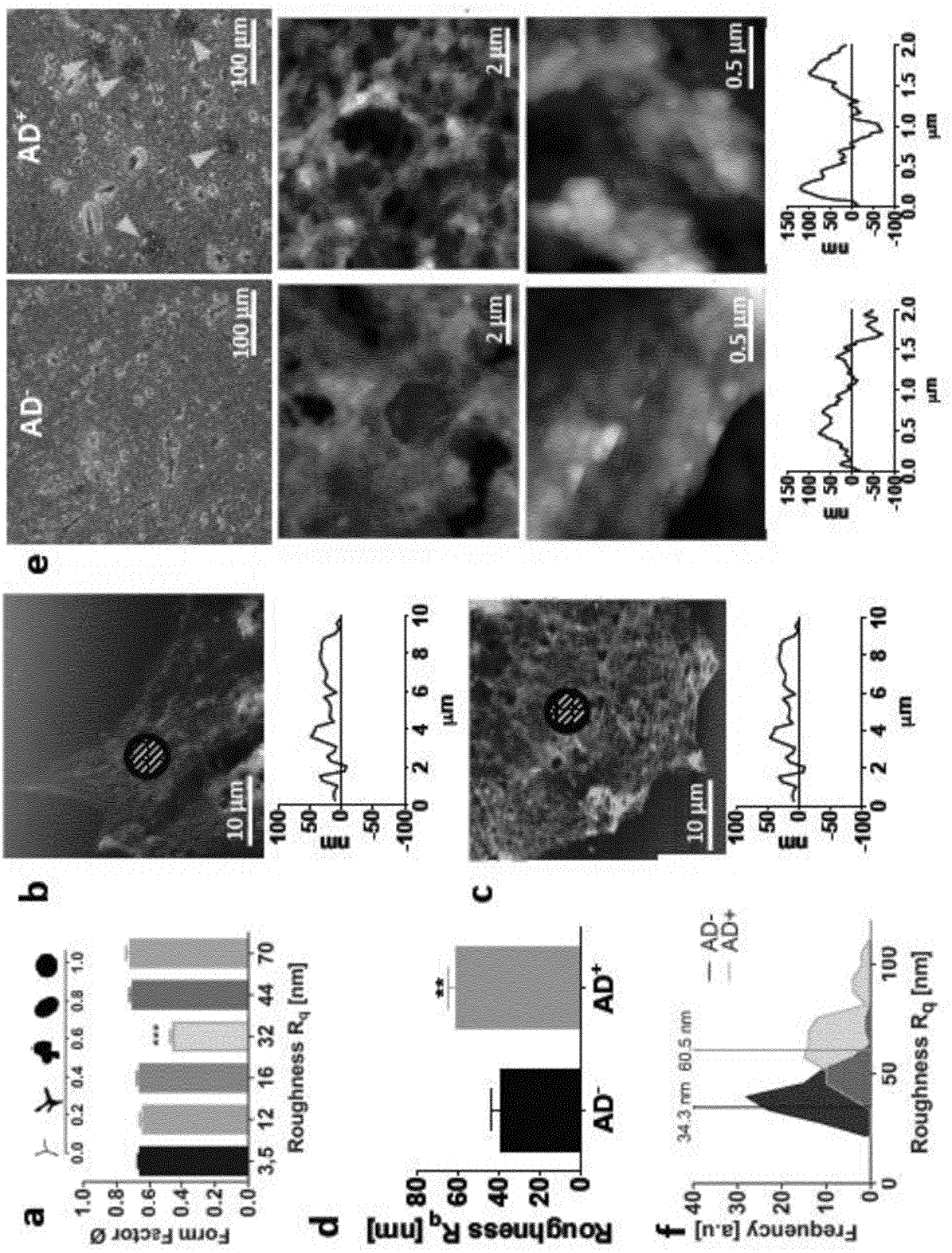
a
Form Factor Ø
Roughness Rq [nm]
b
10 µm
µm
c
10 µm
µm
d
Roughness Rq [nm]
AD-
AD+
e
AD-
AD+
100 µm
2 µm
0.5 µm
µm
f
Frequency [a.u]
34.3 nm
60.5 nm
— AD-
— AD+
Roughness Rq [nm]

REFERENCES CITED IN THE DESCRIPTION

This list of references cited by the applicant is for the reader's convenience only. It does not form part of the European patent document. Even though great care has been taken in compiling the references, errors or omissions cannot be excluded and the EPO disclaims all liability in this regard.

Patent documents cited in the description

- WO 2014116132 A **[0007]**

Non-patent literature cited in the description

- **AM LIPSKI ; C PINO ; FR HASELTON ; I-W. CHEN ; VP SHASTRI.** The effect of silica nanoparticle-modified surfaces on cell morphology, cytoskeletal organization and function. *Biomaterials,* 2008, vol. 3836 (28 **[0004]**
- **PENNISI CP ; DOLATSHAHI-PIROUZ A ; FOSS M ; CHEVALLIER J ; FINK T ; ZACHAR V ; BESENBACHER F ; YOSHIDA K.** Nanoscale topography reduces fibroblast growth, focal adhesion size and migration-related gene expression on platinum surfaces. *Colloids Surf B Biointerfaces,* 01 July 2011, vol. 85 (2), 189-97 **[0005]**
- **SEIL ; WEBSTER.** Decreased astroglial cell adhesion and proliferation on zinc oxide nanoparticle polyurethane composites. *Int J Nanomedicine,* December 2008, vol. 3 (4), 523-531 **[0006]**
- **THEODOSIS D ; POULAIN D ; OLIET S.** Activity-dependent structural and functional plasticity of astrocyte-neuron interactions. *Physiol Rev,* 2008, 983-1008 **[0010]**
- **WADE JJ ; MCDAID LJ ; HARKIN J ; CRUNELLI V ; KELSO J A S.** Bidirectional coupling between astrocytes and neurons mediates learning and dynamic coordination in the brain: a multiple modeling approach. *PLoS One,* 2011, vol. 6, e29445 **[0010]**
- **JOHNSON ; JOHNSON ; PFIZER.** *in Phase III clinicals,* July 2014 **[0014]**
- **SATOH K ; HATA M ; TAKAHARA S ; TSUZAKI H ; YOKOTA H ; AKATSU H ; YAMAMOTO T ; KOSAKA K ; YAMADA T.** A novel membrane protein, encoded by the gene covering KIAA0233, is transcriptionally induced in senile plaque-associated astrocytes. *Brain Res.,* 07 September 2006, vol. 1108 (1), 19-27 **[0015]**
- **ZHONG Y ; BELLAMKONDA RV.** Biomaterials for the central nervous system. *J R Soc Interface,* 06 September 2008, vol. 5 (26), 957-75 **[0022]**
- **FERNÁNDEZ-KLETT F ; PRILLER J.** The fibrotic scar in neurological disorders. *Brain Pathol,* July 2014, vol. 24 (4), 404-13 **[0024]**
- **ASPLUND M ; BOEHLER C ; STIEGLITZ T.** Anti-inflammatory polymer electrodes for glial scar treatment: bringing the conceptual idea to future results. *Front Neuroeng.,* 13 May 2014, vol. 7, 9 **[0028]**
- **LIPSKI AM ; PINO CJ ; HASELTON FR ; CHEN I-W ; SHASTRI VP.** The effect of silica nanoparticle-modified surfaces on cell morphology, cytoskeletal organization and function. *Biomaterials,* 2008, vol. 29, 3836-46 **[0041]**
- **LIPSKI A. M et al.** Nanoscale Engineering of Biomaterial Surfaces. *Adv Mater,* 2007, vol. 19, 553-557 **[0041]**
- **SHASTRI VP.** In vivo engineering of tissues: Biological considerations, challenges, strategies, and future directions. *Adv Mater,* 2009, vol. 21, 3246-54 **[0041]**
- **GREENE L ; TISCHLER S.** Establishment of a noradrenergic clonal line of rat adrenal pheochromocytoma cells which respond to nerve growth factor. *Proc Natl Acad Sci U S A,* 1976, vol. 73, 2424-8 **[0042]**
- **CUI W ; ALLEN ND ; SKYNNER M ; GUSTERSON B ; CLARK A J.** Inducible ablation of astrocytes shows that these cells are required for neuronal survival in the adult brain. *Glia,* 2001, vol. 34, 272-82 **[0047] [0051]**
- **AM LIPSKI ; C PINO ; FR HASELTON ; I-W. CHEN ; VP SHASTRI.** The effect of silica nanoparticle-modified surfaces on cell morphology, cytoskeletal organization and function. *Biomaterials,* 2008, vol. 28, 3836 **[0048]**
- **FRICKER R A et al.** Site-specific migration and neuronal differentiation of human neural progenitor cells after transplantation in the adult rat brain. *J Neurosci,* 1999, vol. 19, 5990-6005 **[0048]**
- **NILIUS B.** Pressing and squeezing with Piezos. *EMBO Rep,* 2010, vol. 11, 902-3 **[0048]**
- **COSTE B et al.** Piezol and Piezo2 are essential components of distinct mechanically activated cation channels. *Science,* 2010, vol. 330, 55-60 **[0048]**
- **ROUDAUT Y et al.** Touch sense: functional organization and molecular determinants of mechanosensitive receptors. *Channels,* 2012, vol. 6, 234-45 **[0048]**
- **DELMAS P ; HAO J ; RODAT-DESPOIX L.** Molecular mechanisms of mechanotransduction in mammalian sensory neurons. *Nat Rev Neurosci,* 2011, vol. 12, 139-53 **[0052]**

- **BAE C ; SACHS F ; GOTTLIEB P.** The mechanosensitive ion channel Piezol is inhibited by the peptide GsMTx4. *Biochemistry,* 2011, vol. 50, 6295-6300 **[0052]**
- **GALTREY CM ; FAWCETT JW.** The role of chondroitin sulfate proteoglycans in regeneration and plasticity in the central nervous system. *Brain Res Rev,* 2007, vol. 54, 1-18 **[0053]**
- **FRASER PE ; LÉVESQUE L ; MCLACHLAN DR.** Alzheimer A beta amyloid forms an inhibitory neuronal substrate. *J Neurochem,* 1994, vol. 62, 1227-30 **[0054]**
- **IVINS KJ ; THORNTON PL ; ROHN TT ; COTMAN CW.** Neuronal apoptosis induced by beta-amyloid is mediated by caspase-8. *Neurobiol Dis,* 1999, vol. 6, 440-9 **[0054]**
- **BUFFO A ; ROLANDO C ; CERUTI S.** Astrocytes in the damaged brain: molecular and cellular insights into their reactive response and healing potential. *Biochem Pharmacol,* 2010, vol. 79, 77-89 **[0055]**
- **WANNER IB et al.** Glial scar borders are formed by newly proliferated, elongated astrocytes that interact to corral inflammatory and fibrotic cells via STAT3-dependent mechanisms after spinal cord injury. *J Neurosci,* 2013, vol. 33, 12870-86 **[0055]**
- **SATOH K et al.** A novel membrane protein, encoded by the gene covering KIAA0233, is transcriptionally induced in senile plaque-associated astrocytes. *Brain Res,* 2006, vol. 1108, 19-27 **[0055]**

专利名称(译)	用于神经元植入物的改进的生物材料，以及所述生物材料在神经元疾病的诊断和治疗中的用途		
公开(公告)号	EP3006055B1	公开(公告)日	2020-02-19
申请号	EP2014188556	申请日	2014-10-10
申请(专利权)人(译)	ALBERT - 路德维希安大学弗莱堡		
当前申请(专利权)人(译)	ALBERT - 路德维希安大学弗莱堡		
[标]发明人	SHASTRI PRASAD BLUMENTHAL NILS R		
发明人	SHASTRI, PRASAD BLUMENTHAL, NILS R.		
IPC分类号	A61L27/50 A61L27/36 A61B5/00 A61N1/05 A61B5/04		
CPC分类号	A61B5/04001 A61B5/4082 A61B5/4088 A61L27/3675 A61L27/50 A61L2400/12 A61N1/0531 A61N1/0536 A61N1/0551 A61B5/04 A61N1/04 G01N33/502 G01N33/5023 G01N33/5058 G01N33/68		
代理机构(译)	KRAUSS，JAN		
其他公开文献	EP3006055A1		
外部链接	Espacenet		

摘要(译)

神经植入物技术领域本发明涉及一种神经植入物，其包括具有外表面具有随机纳米粗糙度（Rq）的生物材料，并且所述随机纳米粗糙度在诊断和/或治疗神经系统疾病例如帕金森氏病中的应用。 ，阿尔茨海默氏病，胶质母细胞瘤和/或在选自PIEZO-1和PIEZO-2离子通道家族的哺乳动物机械感测离子通道的背景下破坏和/或预防神经胶质疤痕。

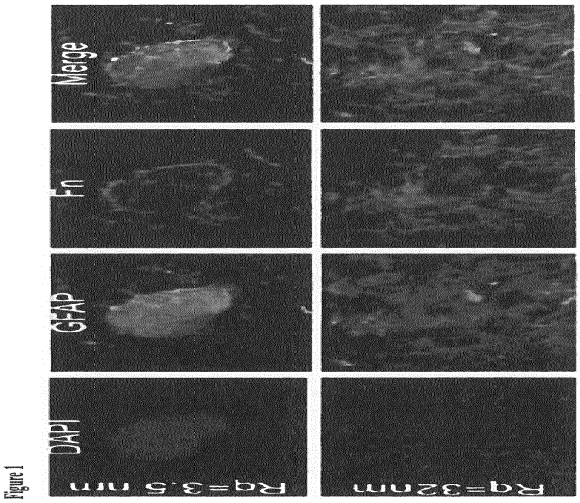

Figure 1